Foaming and emulsifying properties of extensively and mildly extracted Bambara groundnut proteins: A comparison of legumin, vicilin and albumin protein

Jack Yang [a], Annemiek de Wit [a], Claudine F. Diedericks [a,b], Paul Venema [a], Erik van der Linden [a], Leonard M.C. Sagis [a,*]

[a] *Laboratory of Physics and Physical Chemistry of Foods, Wageningen University, Bornse Weilanden 9, 6708, WG, Wageningen, the Netherlands*
[b] *Royal Bel Leerdammer B.V., Steenovenweg 4, 4145, KK, Schoonrewoerd, the Netherlands*

ARTICLE INFO

ABSTRACT

Bambara groundnut (BGN) is a novel plant protein source, which has not received much attention in terms of the structure-function relation of its proteins in foaming and emulsifying properties. In this study, these functional properties were evaluated for two BGN protein concentrates that have been extracted using different extraction methods. The first method is based on conventional "extensive" purification, which includes pre-processing (dehulling, defatting and milling), two centrifugation steps and isoelectric point precipitation. The second method is a more sustainable "mild" purification, which does not require pre-processing and uses only one centrifugation step. The three major protein fractions in BGN (vicilin, legumin and albumins) were also purified and included in this study. Both extensively and mildly purified protein concentrates showed comparable emulsion stabilising properties, with emulsions stable against coalescence, flocculation and creaming, for at least seven days. A more pronounced difference was found in the foaming properties, with the mildly purified protein concentrate forming up to 9x more foam, with much higher stability (about 8x higher), compared to the extensively purified protein concentrate. This was attributed to the albumins, which were only present in the mildly purified protein concentrate. These albumins had the ability to form stiff viscoelastic solid-like air-water interfaces, with high dilatational moduli up to 90 mN/m; close to that of whey protein-stabilised interfaces. These strong interfaces largely contributed to the excellent foaming properties of the mildly purified protein extract. We conclude that BGN proteins have promising functional properties, and that mild purification further enhances their potential.

1. Introduction

Plant-based foods are rapidly emerging in the global food market, and for that reason, there is a growing interest in exploiting novel plant sources to obtain plant-based ingredients. An emerging source is the pulse crop Bambara groundnut (BGN) (*Vigna subterranea* (L.) Verdc.), which is extensively cultivated in Africa and also widely grown in some areas in Asia, Northern Australia, and South America (Diedericks, de Koning, Jideani, Venema, & van der Linden, 2019). A major advantage of this crop is its high tolerance to low soil fertility and drought (Arise, Nwachukwu, Aluko, & Amonsou, 2017). Mature BGN seeds contain about 15–25% (w/w) proteins, 54–70% (w/w) saccharides (mainly starch) and 5–7% (w/w) lipids depending on the cultivar (Murevanhema

& Jideani, 2013). The proteins in BGN are also rich in essential amino acids, which are often insufficiently present in plant proteins (Arise et al., 2017). Additionally, the BGN proteins possess promising structural functionalities such as the formation of gels, which have been studied extensively (Adeleke, Adiamo, & Fawale, 2018; Diedericks et al., 2019; Diedericks, Shek, Jideani, & Venema, 2020; Diedericks, Venema, Mubaiwa, Jideani, & van der Linden, 2020; Mubaiwa, Fogliano, Chidewe, & Linnemann, 2018). On the other hand, fewer studies exist on other functional properties such as foam and emulsion stabilisation (Arise et al., 2017; Mubaiwa et al., 2018), with a lack of extensive characterisation of the interface-stabilising properties. As such, this work largely focussed on the interface, foam and emulsion stabilising properties of BGN protein extracts.

---

* Corresponding author.
  E-mail addresses: jack.yang@wur.nl (J. Yang), leonard.sagis@wur.nl (L.M.C. Sagis).

Three major types of storage proteins are present in BGN, which are the globulins comprising of vicilin and legumin, and the albumins (Adebowale, Schwarzenbolz, & Henle, 2011; Diedericks et al., 2019). These proteins were classified based on their solubility using the Osborne classification method (Osborne, 1924). Globulins are known to be soluble in dilute saline solutions and often have an isoelectric point between pH 4 and 5 (Chéreau et al., 2016). The quaternary structure of globulins is also largely affected by system conditions, as globulins exist as monomers, trimers or hexamers at different pH or ionic strength (Gonzalez-Perez & Vereijken, 2007). The proteins vicilin and legumin are often reported to be present in BGN protein extracts (Arise et al., 2017; Diedericks et al., 2019; Diedericks et al., 2020). Another group of plant proteins are the water-soluble albumins, which remain soluble at a wide pH range, such as demonstrated for albumins from sunflower seeds that remained soluble between pH 2 and 9 (Gonzalez-Perez, Vereijken, van Koningsveld, Gruppen, & Voragen, 2005).

The type of protein obtained in a protein extract can be tuned using the solubility of the proteins. Currently, plant proteins (including from BGN) are extracted using a conventional wet protein extraction. First, the plant source is pre-processed, which include steps such as dehulling, milling and defatting. The material is solubilised at alkaline pH (pH 8–10) to increase the solubility of the globulins, as the pH is far from the isoelectric point of the proteins (Sari, Mulder, Sanders, & Bruins, 2015). In the next step, solids are removed through, e.g. centrifugation, to obtain the soluble fraction, which contains soluble globulin and albumins but also other solutes such as phenols and sugars. The latter can be removed by adjusting the pH to the isoelectric point of the globulins, followed by centrifugation. The pellet with globulins is further processed into the plant protein concentrate/isolate, whilst the supernatant containing albumins and other solutes is discarded. This is unfortunate, as albumins were found to possess interesting functional properties, such as foam stabilisation (González-Pérez, Vereijken, Van Koningsveld, Gruppen, & Voragen, 2005; Guéguen et al., 1996; Lu, Quillien, & Popineau, 2000).

Another disadvantage of the conventional purification method is the extensive processing steps, which reduce the sustainability aspect of the plant source. Additionally, the pH shift to precipitate the globulins resulted in decreased protein solubility and promoted aggregate formation (Jiang, Chen, & Xiong, 2009; Kornet et al., 2020). These challenges can be avoided by performing mild purification methods (Geerts, Nikiforidis, van der Goot, & van der Padt, 2017). Ntone et al. demonstrated a wet extraction method to produce a rapeseed protein concentrate, without pre-processing steps (e.g. defatting and milling) and isoelectric point precipitation (Ntone, Bitter, & Nikiforidis, 2020). Smaller solutes such as small saccharides, phenols and salts were removed using diafiltration. The disadvantage of mild purification is the lower protein purity, which was 65% (w/w) in the case of the rapeseed protein concentrate, which still contained about 15% (w/w) of lipids. Our previous work demonstrated excellent foam stabilising properties of a mildly purified rapeseed protein concentrate containing about 8% (w/w) lipids (Yang et al., 2020). Another component present in this extract is the albumins, which are removed in conventional extensive protein extraction methods.

In this work, BGN protein concentrates were obtained from both the conventional extensive purification and the more sustainable mild purification method. To further study the contribution of the different proteins present in BGN, the vicilin, legumin and albumins were also obtained through the Osborne fractionation method. These protein extracts and fractions were studied in for their physico-chemical properties (composition, structure nativity and surface properties), which were linked to the air-water interface, foam and emulsion stabilising properties. Here, we aim to present a more sustainable option to extract proteins from a plant source, such as BGN. The novel element of the current work is the inclusion of the separate protein fractions (vicilin, legumin and albumin), which helps us understand the contribution of each individual protein in interface, foam and emulsion stabilisation.

Such understanding could allow the design of protein extracts with promising functional properties in multiphase systems, leading to a more effective and sustainable utilisation of plant proteins.

2. Experimental section

2.1. Materials

Bambara groundnut (BGN) seeds were purchased from Thusano Products (Louis Trichardt, Limpopo, South Africa). Mixed varieties of BGN were used in this study. The seeds were screened for defects and foreign materials before selection for further processing. The SDS-PAGE materials (Invitrogen Novex, ThermoFisher, USA) and other chemicals (Sigma-Aldrich, USA) were used as received. Rapeseed oil was provided by Danone Nutricia Research (The Netherlands). Ultrapure water (MilliQ Purelab Ultra, Germany) was used for all experiments.

2.2. Sample preparation

2.2.1. Preparation of defatted BGN flour

This method was obtained from Diedericks et al. with some adaptations (Diedericks, Venema, et al., 2020). The 1 kg of sorted BGN seeds was soaked in MilliQ water for 16 h to weaken the hull. Afterwards, the water was discarded, and the seeds were dried in an oven at 40 °C for 24 h. The seeds were dehulled with a combination of automatic (grain testing mill, TM-05, Satake Engineering, Japan) and manual dehulling. Afterwards, the dehulled seeds were coarse-milled using an LV 15M pin mill (Condux-Werk, Germany). The coarse-milled seeds were defatted with n-Hexane in a seed to hexane ratio of 1:3 (w/v) at room temperature. The seeds were stirred for 2 h, followed by decanting of the hexane. These washing steps were repeated twice. After the final wash step, the mixture was passed through a paper filter to remove the hexane, and the retentate was dried overnight under a stream of nitrogen gas. The defatted BGN was fine-milled with a Pulverisette 14 rotor mill (Fritsch GmbH, Germany) equipped with a 0.5 mm mesh sieve ring, whilst constantly cooled with liquid nitrogen. The fine flour was sieved through a 315 μm mesh sieve using an E200 LS air jet sieve (Hosokawa Alpine, Germany). Finally, 700 g of defatted BGN flour was obtained and stored at −20 °C until further use.

2.2.2. Preparation of extensively purified BGN protein concentrate

The protein extraction method was obtained from Diedericks et al. (Diedericks, Venema, et al., 2020) with some adaptations and is depicted in Fig. 1. The defatted BGN flour (400 g) was dispersed in MilliQ water in a 1:10 (w/w) ratio. The pH was adjusted to 9.5 using 1M NaOH. The sample was stirred for 2 h, and the pH was continuously adjusted to 9.5. After 2 h, the mixture was centrifuged for 30 min at 4,000×g. The supernatant was adjusted to pH 4.0 using 1M HCl and stirred for 1 h, whilst continuously adjusting the pH to 4.0. This mixture was centrifuged for 30 min at 4,000×g, and the supernatant and pellet were separated. The pellet was weighed and resuspended in MilliQ water in a 1:5 (w/w) ratio. The pH was adjusted to pH 7.0, and the sample was stirred for 2 h, whilst continuously adjusting the pH to 7.0. The resuspended pellet was freeze-dried and labelled as the extensively purified BGN protein concentrate (EP-BGC), of which 82 g was obtained. All samples were stored at −20 °C until further use.

2.2.3. Preparation of mildly purified BGN protein concentrate

The mild purification method was obtained from Ntone et al. with several adaptations and depicted in Fig. 1(N–ne et al., 2020). A total of 840 g of intact BGN seeds (with hull) were coarse-milled using an LV 15M pin mill (Condux-Werk, Germany). The milled seeds were dispersed in MilliQ water at a ratio of 1:7 (w/w) and stirred for 1 h. After stirring, the hulls of about half of the seeds were detached due to the soaking and shear of the stirrer. These hulls were removed from the suspension, and the pH was adjusted to pH 9.5, followed by 2.5 h stirring, whilst
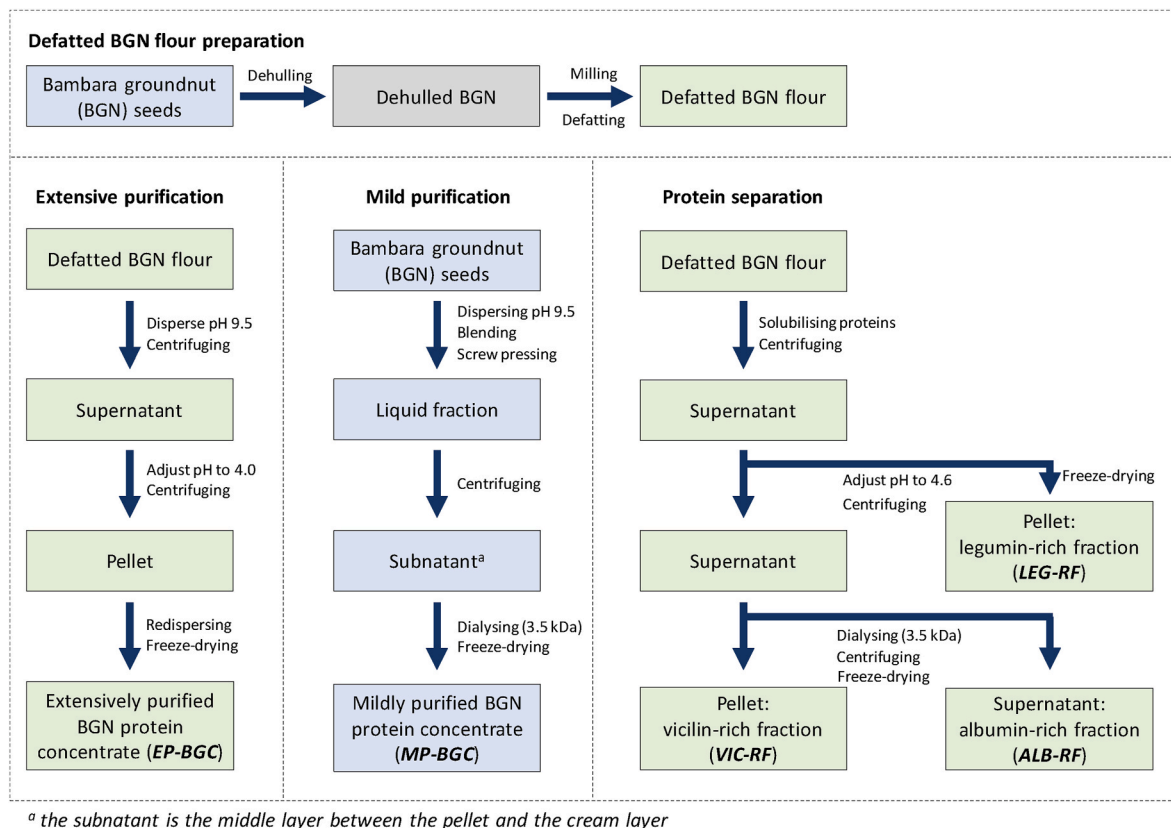
Fig. 1. Overview of protein extraction processes applied in this work.

continuously adjusting the pH to 9.5. The mixture was blended in a Vita-Prep blender (Vitamix, USA) at max speed for 2 min. The slurry's pH was adjusted to 9.5 and stirred for another 30 min, whilst constantly adjusting the pH to 9.5. The solids and supernatant were separated with a twin-screw press, and the pH of the supernatant was adjusted to 9.5. The supernatant was centrifuged at $10,000 \times g$ for 30 min (4 °C), which resulted in a three-layer system: a pellet with solids, a middle layer (subnatant) with proteins and other solutes, and a top layer with cream. The subnatant was recovered and dialysed in Spectrum Spectra/Por 3 RC dialysis tubes (Thermo Fisher, USA) with a 3.5 kDa cut-off at 4 °C to remove salts and free phenols. The dialysate (demineralised water) was exchanged until the conductivity remained constant (five water exchanges). The dialysed sample was freeze-dried and labelled as mildly purified BGN protein concentrate (MP-BGC), of which 174 g was obtained. The MP-BGC was stored at −20 °C until further use.

2.2.4. Separation of vicilin, legumin and albumin proteins

The different plant protein groups present in BGN were separated using an Osborne fractionation method (Diedericks et al., 2019). A schematic overview can be found in Fig. 1. The defatted BGN flour (110 g) was dispersed in 0.5 M NaCl at a 1:10 (w/w) ratio and stirred for 1 h. The mixture was centrifuged for 20 min at $10,000 \times g$. The pellet was resuspended, stirred and centrifuged twice, of which the final extraction step was performed with MilliQ water instead of 0.5 M NaCl. The three supernatants from the centrifugation steps were pooled, and contained a mixture of BGN vicilins, legumins, albumins and other solutes. The pooled supernatants were adjusted to pH 4.6 with glacial acetic acid to precipitate legumin. After 30 min of stirring, the mixture was centrifuged. The pellet was resuspended in MilliQ water in a 1:5 (w/w) ratio, and the pH was adjusted to 7.0 with 1 M NaOH, followed by 1 h stirring and finally freeze-drying. The supernatant containing the other soluble proteins (vicilin and albumin) were dialysed in Spectrum Spectra/Por 3 RC dialysis tubes (Thermo Fisher, USA) with a 3.5 kDa cut-off at 4 °C to

remove salts and low molecular weight sugars. The dialysate (demineralised water) was exchanged until the conductivity remained constant (five water exchanges). Removal of salt resulted in the aggregation of vicilin, which could be separated from albumins by centrifugation. The supernatant containing albumins was adjusted to pH 7.0 and freeze-dried. The pellet containing vicilin was resuspended in MilliQ water in a 1:5 (w/w) ratio, and the pH was adjusted to 7.0, followed by 2 h stirring, before the vicilin was freeze-dried. The vicilin (10 g obtained), legumin (7 g obtained) and albumin-rich (4 g obtained) fractions are abbreviated as VIC-, LEG- and ALB-rich fractions (RF), respectively.

2.2.5. Preparation of protein solutions

Protein samples in this work were dissolved based on protein concentration (% w/w) in a sodium phosphate buffer (20 mM, pH 7.0) and stirred for 4 h at room temperature. All samples were freshly prepared for all measurements and discarded after 24 h.

2.3. Composition analysis

2.3.1. Protein content

Protein content was measured by determining the nitrogen content of at least three triplicates using a Flash EA 1112 Series Dumas (Interscience, The Netherlands). The nitrogen content was converted into protein content by using a conversion factor of Nx5.7. Protein yields were calculated by expressing the total amount of protein in the extract (amount of extract times protein content) to the amount of protein in the start material (amount of start material times protein content).

2.3.2. Lipid content

The lipid content was measured in triplicate by a Soxhlet extraction of 6 h using petroleum ether as a solvent. The final lipid content was determined by weighing the starting material and the oil in the collection flasks after solvent evaporation in a rotor evaporator.

2.3.3. Starch content

The starch content was measured using an enzyme starch kit (Megazyme Inc., Ireland). First, smaller saccharides were removed using ethanol and centrifugation steps. Afterwards, the starch was enzymatically digested using α-amylase and amyloglucosidase. The products of the enzyme reaction were mixed with p-hydroxybenzoic reagent, glucose oxidase and peroxidase. The mixtures were measured for their absorbance at a wavelength of 510 nm, including D-glucose and maise starch standards. Each sample was prepared separately in triplicate, and each replicate was diluted into two separate samples before absorbance measurements.

2.3.4. Phenol content

The phenol content was determined using a Folin-Ciocalteu assay. A calibration curve of tannic acid was prepared by dissolving in MilliQ water in a concentration range of 0.001–0.01% (w/w). Similarly, the samples were dissolved in MilliQ water at concentrations between 0.01 and 0.5% (w/w). Aliquots of 0.5 mL of the samples were diluted with 2.5 mL of MilliQ water, followed by the addition of 0.25 mL Folin-Ciocalteu reagent and mixing by vortexing. Finally, 0.5 mL of a saturated Na_2CO_3 solution was added and the total sample volume adjusted to 5 mL with MilliQ water. The samples were incubated at room temperature for 1 h and vortexed again before measuring the absorbance at 725 nm. All samples were prepared in duplicate.

2.3.5. Ash content

The ash content was determined in duplicate by igniting the samples in an oven at 550 °C for 24 h, followed by cooling of samples in a desiccator. The weight of the samples before and after drying was used to determine the ash content.

2.4. Protein composition by SDS-PAGE

Solutions containing 0.1% protein (w/w) were prepared in MilliQ water, and were mixed with 500 mM DTT and NuPAGE LDS sample buffer. The mixtures were heated for 10 min at 70 °C and were loaded on a 4–12% (w/w) BisTris gel. A molecular weight marker with a range of 2.5–200 kDa was also included. Finally, an electrophoresis step was performed at 200 V for approx. 30–35 min. Protein staining was done with SimplyBlue Safestain, before the gels were scanned in a gel scanner.

2.5. Determination of particle size and zeta-potential

The particle size and zeta-potential of 0.01% (w/w) protein solutions were determined using dynamic light scattering in a Zetasizer Nano ZS (Malvern Instruments, UK). The refractive indices for proteins and the water phase were set at 1.45 and 1.33, respectively. All measurements were performed at least in triplicate at 20 °C.

2.6. Determination of protein surface hydrophobicity

The protein surface hydrophobicity was determined using a fluorescence agent 8-anilino-1-napthalenesulfonic acid ammonium salt (ANSA). The protein samples were dissolved in a protein concentration range of 0.005–0.04% (w/w). Cuvettes (4 mL capacity) were filled with 3 mL protein solution and 25 μl of an 8 mM ANSA solution. The cuvettes were carefully rotated to mix the solutions and incubated in the dark for 1 h at room temperature. The fluorescence spectra were measured using an LS 50B luminescence spectrometer (PerkinElmer, USA) at an excitation and emission wavelength of 390 nm and 470 nm, respectively. A buffer solution with ANSA was included as a blank. The slope of the fluorescence intensity versus the protein concentration was determined as the protein surface hydrophobicity. Two independent samples were prepared, and each replicate was measured twice.

2.7. Determination of protein denaturation properties

The protein denaturation properties were determined by differential scanning calorimetry in a Q100 DSC (TA Instruments, USA). About 50 mg of each 10% protein (w/w) solution was added to a stainless steel high volume pan. The samples were equilibrated at 20 °C for 5 min and heated to 140 °C at a rate of 5 °C/min. Finally, the samples were cooled to 20 °C at a rate of 10 °C/min to evaluate potential protein refolding. The samples were measured in triplicate.

2.8. Determination of air-water interfacial properties

Interfacial properties were determined using a drop tensiometer PAT-1M (Sinterface Technologies, Germany). A sample solution with 0.1% protein (w/w) was injected through a needle to form a hanging droplet at the needle tip. The surface area was stabilised at 20 mm^2, and the shape of the droplet was analysed with the Young-Laplace equation to determine the surface tension. The area of the droplet was maintained in a waiting step of 3 h before the interface was subjected to dilatational deformation. Frequency sweeps were performed, where the frequency increases from 0.002 to 0.1 Hz at a fixed amplitude of 3%. Amplitude sweeps were performed, where the amplitude increases from 3 to 30% at a fixed frequency of 0.02 Hz. Five oscillatory cycles were performed at each frequency or amplitude. Step-dilatation experiments were performed by a rapid 10% area increase (extension) or decrease (compression), with a step time of 2 s. These measurements were performed at least in triplicate at 20 °C.

2.9. Interfacial rheological data analysis

Lissajous plots of the oscillatory amplitude sweeps were constructed by plotting the surface pressure ($\Pi = \gamma\text{-}\gamma_0$) over the deformation (($A\text{-}A_0$)/A_0). Here γ and A are the surface tension and area of the deformed interface of the droplet, γ_0 and A_0 are the surface tension and area of the non-deformed interface. From the five oscillations cycles, the middle three oscillations of each amplitude were used to construct the plots.

2.10. Determination of foam properties

2.10.1. Foam ability

The foamability was determined by whipping 15 mL of each protein solution (0.1 and 1% w/w) for 2 min at 2000 rpm using an aerolatte froth (Aerolatte, UK) connected to an overhead stirrer. The samples were whipped in plastic tubes (ø = 3.4 cm), and after whipping, the top of the foams was directly marked on the tubes. The foam height was measured with a ruler. The foam height and tube diameter were used to determine the foam volume. From this, the overrun (%) was determined by the foam volume (mL) divided by the liquid volume (15 mL) times 100. All experiments were performed in triplicate at room temperature.

2.10.2. Foam stability

The foam stability of solutions containing 0.1 and 1% (w/w) protein was determined using a sparging method in a Foamscan (Teclis IT-Concept, France). A glass cylinder (ø = 60 mm) was filled with 40 mL of sample. Nitrogen gas was sparged through a metal frit (27 μm pore size, 100 μm distance between centres of pores, square lattice) at a gas flow rate of 400 mL/min to a foam volume of 400 mL. A camera monitored the foam volume until half of the foam volume collapsed. The time to reach this point is referred to as the foam volume half-life time. Detailed images of air bubbles were recorded with an SLR lens. These images were analysed using DIPlip and DIPimage image analysis (TU Delft, the Netherlands) to obtain an average bubble size. All foaming experiments were performed at least in triplicate at 20 °C.

2.11. Determination of emulsifying properties

2.11.1. Rapeseed oil stripping

Rapeseed oil was stripped to remove surface active impurities using magnesium silicate (Florisil 100–200 mesh, Sigma-Aldrich, USA). Florisil was dispersed in rapeseed oil in a ratio of 1:2 (v/v) (Florisil:oil) in airtight tubes, and covered in aluminium foil to avoid air and light oxidation. The tubes were rotated overnight in a vertical rotor at room temperature. Afterwards, the mixture was centrifuged at $2,000 \times g$ for 20 min to remove the Florisil. The supernatant was again subjected to centrifugation to obtain the purified rapeseed oil, before storage at $-20\,°C$.

2.11.2. Preparation of oil-in-water emulsions

Oil-in-water emulsions were produced with 0.2–2% (w/w) protein solutions, and stripped rapeseed oil was added to obtain a 10% (w/w) oil content. The samples were mixed with an Ultra-Turrax (IKA, USA) at 12,000 rpm for 1 min to obtain a pre-emulsion, which was homogenised at 200 bar for 10 passes using a LAB high-pressure homogeniser (Delta Instruments, The Netherlands).

2.11.3. Determination of emulsion droplet size

The droplet size of the emulsions was studied using static light scattering in a Mastersizer 2000 (Malvern Instruments Ltd, UK). The droplet size was determined directly after emulsion production (day 0), after one day (day 1) and seven days (day 7), whilst stored at 4 °C before measurement. Droplet flocculates were broken up by mixing emulsions and a 1% (w/w) sodium dodecyl sulphate (SDS) solution in a 1:1 (v/v) ratio, and these samples were also measured for the droplet size. Refractive indices of 1.469 and 1.330 were used for the dispersed phase (rapeseed oil) and dispersant (demineralised water), respectively. All measurements were performed in triplicate.

2.11.4. Determination of emulsion creaming

The creaming rate of the emulsions was assessed by adding 10 mL of the emulsions into a 15 mL tube, directly after emulsion formation. The tubes were evaluated on day 0, 1 and 7 by using a light source to evaluate the presence of a creamed layer.

2.12. Statistical analysis

Analysis of variance was performed on the data set using an ANOVA (one-way analysis of variance) and Duncan's test at $p \leq 0.05$ to evaluate the statistical significance between samples. The tests were run in SPSS 25.0 (SPSS Inc., USA).

3. Results and discussion

3.1. Protein extraction

The Bambara groundnut (BGN) seeds were processed by soaking to soften the hulls, coarse grinding and dehulling. First, the dehulling was performed using an automated dehulling device, which removed approximately one-third of the hulls, and the remaining hulls were removed manually. The dehulled BGN seeds had a protein content of 17.4% (w/w), and were further processed by defatting using hexane to obtain a defatted BGN flour with 20.5% (w/w) protein. The defatted BGN flour was used in the conventional extensive purification method, and yielded an extensive purified BGN protein concentrate (EP-BGC). In the mild purification method, the coarsely ground BGN seeds, including hulls, were soaked and stirred using an overhead stirrer. The combination of soaking and stirring detached a portion (~50%) of the hulls, which were removed. In the next steps, the (partially) dehulled seeds were blended, and solids were removed using a twin-screw press and centrifugation. The centrifugation also resulted in a thin cream layer on top, which was carefully removed. The subnatant containing the solutes

was dialysed to remove smaller solutes, such as sugars, phenols and minerals, to obtain the mild purified BGN protein concentrate (MP-BGC). A schematic overview of both extraction processes is depicted in Fig. 1.

The composition of the EP-BGC and MP-BGC is shown in Table 1. The EP-BGC and MP-BGC have a protein content of 78.8% (w/w) and 62.1% (w/w), respectively. The protein yield was determined by dividing the amount of protein extracted over the amount of protein in the starting material times 100, and was comparable for both concentrates, which was 79.8% for EP-BGC, and 77.4% for MP-BGC. The lower protein content of MP-BGC is due to the presence of more non-proteinaceous compounds such as lipids, phenols and starch. The MP-BGC has a lipid content of 10.8%, whilst the EP-BGC contained only 0.6% lipids. The lipids in the MP-BGC are in the form of oleosomes, which are the natural lipid storage organelles in plants. The oleosome is a triglyceride droplet surrounded by a phospholipid/protein membrane; the membrane gives the surface of the oleosomes a hydrophilic character, as the hydrophilic parts of the phospholipids and membrane proteins are directed outwards (Nikiforidis, 2019). The centrifugation step in the mild purification method removes a portion of the oleosomes in the top cream layer. However, since oleosomes can have a diameter as small as 200 nm, some of these smaller ones can remain in the subnatant layer. This was also observed for mildly purified rapeseed protein concentrates using a comparable extraction method (Ntone et al., 2020).

Phenols are another component present in BGN, with the MP-BGC having about two times more phenols than EP-BGC. This was as expected, considering that the BGN seed hulls contain high amounts of phenols, especially tannins and flavonoids, which will be extracted into the MP-BGC (Harris, Jideani, & Le Roes-Hill, 2018). Even though the MP-BGC was diafiltrated, the phenol content was still higher, which could be attributed to interactions between phenols and proteins (Shahidi & Senadheera, 2019). These could be non-covalent interactions of the hydrophobic benzene ring of phenols with the hydrophobic regions on the protein surface (Jin et al., 2012). Covalent interactions between phenols and proteins might also occur due to phenol oxidation at the alkaline pH of 9.5 in the protein extraction. Oxidised phenols are highly reactive and can interact with free thiol and amino groups on proteins, thus forming covalent bonds (Keppler, Schwarz, & van der Goot, 2020). The higher phenol content was also reflected in the colour of the concentrates, as the phenols from the hull resulted in a brown MP-BGC, whilst the EP-BGC was lighter in colour (Fig. 2).

On the other hand, a clear advantage of the mild purification method is the absence of the dehulling step, which is a laborious process requiring (in this study) 16 man-hrs to dehull about 1 kg BGN. The hard-to-cook/hard-to-mill properties of BGN seeds are often associated with the limited use of the crop, with pre-treatments such as soaking and roasting often required to soften the hulls (Mubaiwa, Fogliano, Chidewe, & Linnemann, 2017). In previous work, we have shown that soaking does not affect the molecular composition or morphology of BGN seeds (Diedericks, Venema, et al., 2020). The diafiltration step was effective in reducing the ash content for MP-BGC compared to EP-BGC and removing smaller sugars, as was also demonstrated for pea protein extracts (Kornet et al., 2020). Finally, the starch content was 1.3% for

Table 1

Composition of extensive (EP-BGC) and mild (MP-BGC) purified BGN protein concentrates based on g/100g dry matter (% w/w). Values are presented as mean ± standard deviations; means within a row with the same superscript letter are not significantly different (p > 0.05). The protein content was determined with a nitrogen conversion factor of Nx5.7.

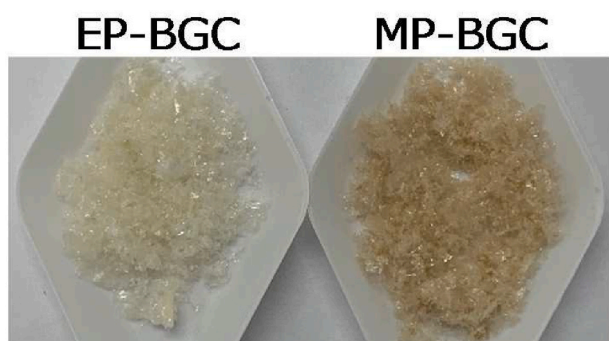|	EP-BGC	MP-BGC
Protein	78.8 ± 0.4[b]	62.1 ± 0.7[a]
Lipid	0.6 ± 0.2[a]	10.8 ± 0.2[b]
Phenol	2.2 ± 0.2[a]	4.2 ± 0.3[b]
Starch	0.2 ± 0.0[a]	1.3 ± 0.2[b]
Ash	6.2 ± 0.3[b]	3.8 ± 0.1[a]

Fig. 2. The visual appearance of extensive (EP-BGC) and mild (MP-BGC) purified BGN protein concentrates.

MP-BGC and 0.2% for EP-BGC. The slightly higher starch content of MP-BGC could be attributed to the soft pellet after centrifugation, whilst the defatted flour formed a solid and firm pellet after the centrifugation step in the EP-BGC extraction. In terms of centrifugation applied in the two extraction methods, the centrifugation force to separate solids was 2.5x lower for EP-BGC compared to MP-BGC. However, the EP-BGC required two centrifugation steps, whilst the MP-BGC only required one step.

The protein fractions in BGN were also extracted and evaluated in relation to the protein concentrates. Fractionation resulted in a vicilin-rich fraction (VIC-RF) with a 91.3% (w/w) protein content, a legumin-rich fraction (LEG-RF) with a 58.9% (w/w) protein content, and an albumin-rich fraction (ALB-RF) containing 57.7% (w/w) protein. An image of the protein extracts can be found in Fig. S1 in the SI. Vicilin was the most abundant protein with a protein yield of 51%, followed by legumin (23%) and albumin (14%). In addition, all extracts were evaluated for structural changes using differential scanning calorimetry, considering that protein structures could be largely affected by the processing steps (Das Purkayastha et al., 2014; Geerts et al., 2017). The

resultant thermograms and thermal transition parameters are shown in Fig. S2 and Table S1 in the SI. All BGN protein extracts showed high denaturation peaks and enthalpies, suggesting the retention of their protein structure. Both protein concentrates (BGCs) showed similar denaturation properties, which were dominated by the vicilin fraction.

3.2. Protein composition

The protein composition of all extracts was further analysed with SDS-PAGE under reducing conditions (Fig. 3). Diedericks et al. showed that BGN vicilin and legumin had a molecular weight of 175 kDa and 385 kDa, respectively (Diedericks et al., 2019). Vicilin occurred in a trimeric form, with their subunits visible as two major bands around 55 kDa. At the same size range between 50 and 60 kDa and around 21 kDa, LEG-RF showed several bands, which are recognised as the legumin subunits. In other pulse crops, such as yellow pea, the legumin fraction is characterised with a β-subunit and an α-subunit, with molecular weights of 20 kDa and 40 kDa, respectively. These legumin subunits are inter-linked by disulphide bonds, which are dissociated under reducing conditions (Barac et al., 2010). In native form, the legumin most likely exists in a hexameric structure. The ALB-RF had visible bands around 4 kDa, 7 kDa and 25 kDa, which are generally attributed to the albumins (light/heavy chains). Both EP-BGC and MP-BGC had bands corresponding to vicilin and legumin, with the vicilin present as the most abundant protein fraction as deduced from the (visual) band intensity. As expected, the albumins were only present in the MP-BGC and not in the EP-BGC, since in the latter, these protein fractions are removed during isoelectric point precipitation.

3.3. Protein size distribution

The size of the BGN protein extracts as analysed with dynamic light scattering is shown in Fig. 4A. The ALB-RF had the smallest size with a peak diameter of around 3 nm. The VIC-RF had a slightly larger peak size around 9 nm, whilst the LEG-RF was characterised with the largest
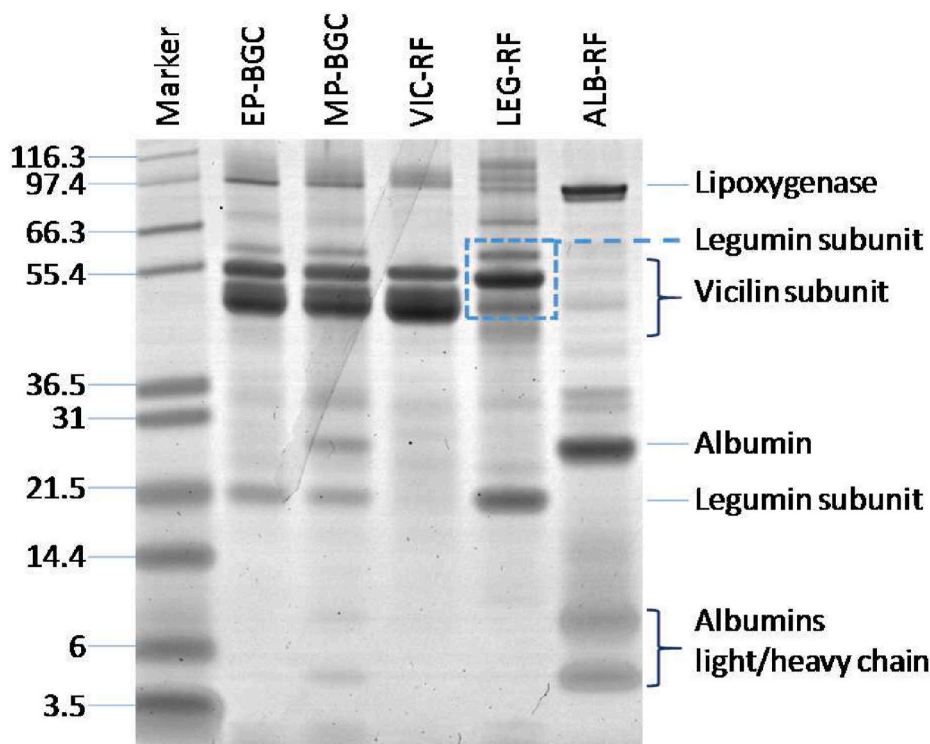

Fig. 3. SDS-PAGE profiles under reducing conditions containing extensively (EP-BGC), and mildly (MP-BGC) purified BGN protein concentrates, vicilin-rich faction (VIC-RF), legumin-rich fraction (LEG-RF), and albumin-rich fraction (ALB-RF). The marker indicating the molecular weights is shown in lane M.
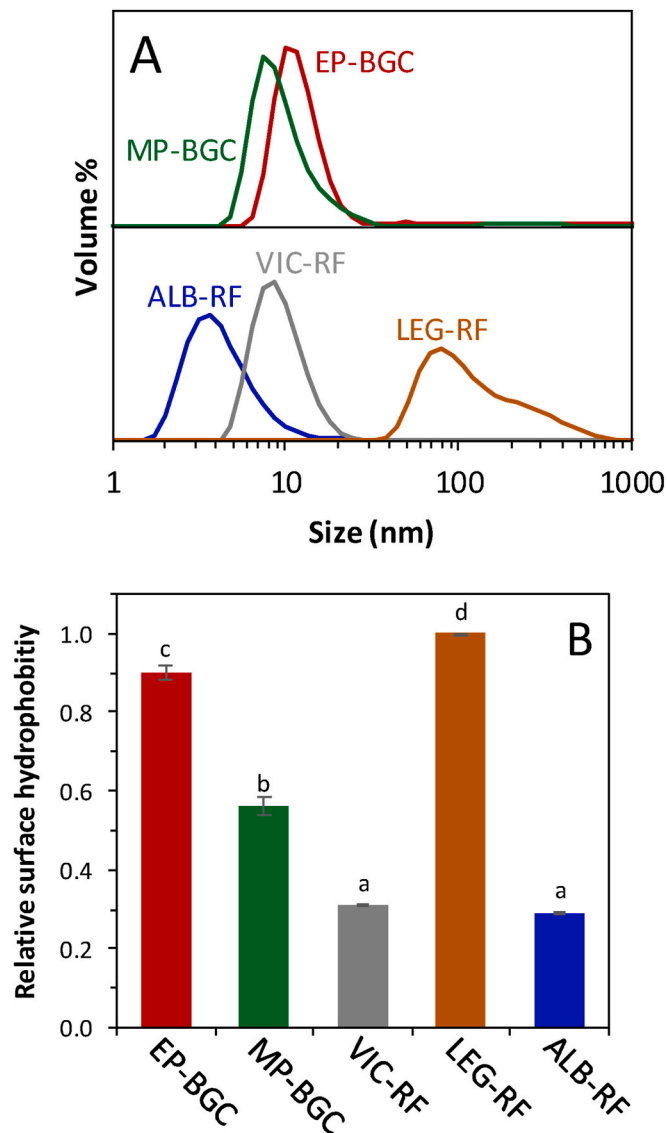
Fig. 4. (A) The size distribution of BGN protein extracts: extensively (EP-BGC) and mildly (MP-BGC) purified concentrates, vicilin-rich faction (VIC-RF), legumin-rich fraction (LEG-RF) and albumin-rich fraction (ALB-RF). For clarity, one representative size distribution measurement is shown for each sample, whilst comparable values were obtained for three replicates. (B) The relative protein surface hydrophobicity of BGN protein extracts. The average and standard error were obtained from four replicates.

particle peak size around 91 nm and a broad size distribution ranging from 40 to 700 nm. These differences in particle sizes were expected based on the SDS-PAGE patterns. However, the large size distribution of the LEG-RF is indicative of the formation of large aggregates. These aggregates could be attributed to the solubility of legumin, which is more saline-dependent compared to the vicilin fraction. The EP-BGC and MP-BGC exhibited a comparable size distribution with peak sizes around 8 and 11 nm, which is also comparable to that of VIC-RF, thus indicating that vicilin is the largest protein fraction in these extracts.

3.4. Protein surface hydrophobicity

The protein surface hydrophobicity was also evaluated by adding a fluorescence probe to the proteins, and these values are depicted in Fig. 4B. The surface hydrophobicity of EP-BGC was roughly 1.5x higher compared to that of MP-BGC. Also here, the difference in protein composition plays a role, considering that albumins are present in MP-

BGC, and as shown for ALB-RF, these proteins had the lowest surface hydrophobicity. Another important factor could also be the non-proteinaceous components, which can interact with hydrophobic regions on the protein surface. Phenols are known to have non-covalent interactions that reduce the protein surface hydrophobicity, and considering the higher phenol content in MP-BGC, these interactions are likely present in these concentrates (Cao, Xiong, Cao, & True, 2018). The main protein fraction, vicilin, showed a lower surface hydrophobicity compared to both concentrates and LEG-RF. From these observations, it can be deduced that the legumins present in EP-BGC and MP-BGC have a large contribution to the protein surface hydrophobicity of these mixtures. The surface hydrophobicity is valuable in interpreting the protein adsorption behaviour, which is further discussed in the following section.

3.5. Interfacial properties

3.5.1. Adsorption behaviour

The surface adsorption behaviour of the BGN protein extracts was assessed with a drop tensiometer (Fig. 5A). The EP-BGC and MP-BGC showed an immediate increase in surface pressure of 15 mN/m,
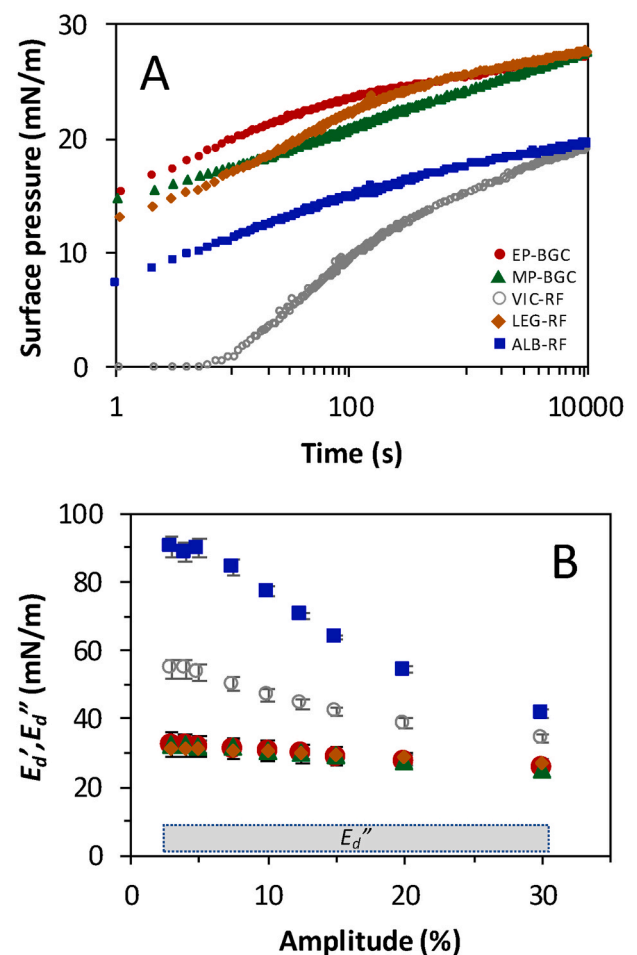

Fig. 5. (A) Surface pressure isotherms of BGN protein extracts: extensively (EP-BGC), and mildly (MP-BGC) purified concentrates, vicilin-rich faction (VIC-RF), legumin-rich fraction (LEG-RF) and albumin-rich fraction (ALB-RF). Each isotherm is an average of at least three replicates. (B) Surface elastic dilatational moduli as a function of deformation amplitude of air-water interfaces, stabilised by BGN protein extracts, measured at an oscillatory frequency of 0.02 Hz. The E_d' is depicted as the symbols, and the E_d'' values were all between 1 and 6 mN/m, and shown in the grey square. Averages and standard deviation of at least three replicates are shown.

followed by an increase over the next 3 h to the same surface pressure of 28 mN/m. MP-BGC had a slower increase in surface pressure in the first 100 s, which can be related to the lower surface hydrophobicity of MP-BGC compared to EP-BGC, as well as the presence of albumins in MP-BGC. The fractionated proteins also showed a distinct adsorption behaviour, with LEG-RF having the fastest increase in surface pressure, similar to EP-BGC and MP-BGC. ALB-RF had a slower increase from 7 to 20 mN/m, whilst VIC-RF had a lag-time of 2 s, followed by an increase to 20 mN/m. The low surface activity of VIC-RF could be attributed to the low surface hydrophobicity (Fig. 4B). ALB-RF showed a faster increase in surface pressure compared to VIC-RF, whilst the surface hydrophobicity was comparable.

Another important parameter to consider here is the molecular size, as vicilin exists in trimers around 170 kDa, and the albumins were found to be around 25 kDa. Also, the distribution of the hydrophilic and -phobic patches on the protein surface is of importance. In rapeseed albumins, for example, it was proposed that these proteins are similar to Janus particles, where two distinct regions exist, a hydrophobic and a hydrophilic one (Ntone et al., 2021). They also showed that these regions are much more evenly distributed on the surface of the rapeseed globulin. Unfortunately, detailed studies on the protein structure of BGN albumins are not available, but albumins from six different sources were previously evaluated for their primary, secondary and tertiary protein structure (Souza, 2020). All sources showed slight differences in their primary protein structure (sequence of amino acids), which did not affect their secondary and tertiary structure. As a result, the three-dimensional structure of these albumins was found to be similar. Therefore, we assumed a comparable structure for BGN and rapeseed albumins. An increased amphiphilicity and smaller molecular size could explain the faster increase of surface pressure for ALB-RF, when compared to VIC-RF in the initial phase of the isotherm. Legumin seems to play an important role in the adsorption behaviour of the BGCs, which was further evaluated with dilatational deformations.

3.5.2. Surface dilatational deformations

The interfaces stabilised with BGN protein extracts were further analysed with amplitude sweeps to evaluate the amplitude dependencies, as shown in Fig. 5B. MP-BGC and EP-BGC-stabilised interfaces had a small decline (32–26 mN/m) in dilatational elastic moduli (E_d'), when increasing the deformation amplitude from 3 to 30%, which suggests a nearly linear behaviour. This low dependence on deformation amplitudes, indicated the formation of a relatively weak and stretchable interfacial layer. LEG-RF had similar moduli values as the concentrates, implying that legumins dominated the layer formation at the surface, which is presumably related to the high surface activity of legumin in comparison to vicilin and albumin. VIC-RF and ALB-RF had higher moduli and an increased amplitude-dependency than the concentrates and LEG-RF, and both were most pronounced for ALB-RF. Albumins formed an interfacial layer with a modulus of 90 mN/m at deformations below 5%, which decreased to 40 mN/m at 30% deformation. These values are remarkably high for plant proteins, almost similar to e.g. whey proteins isolate, which is an excellent interface stabiliser, as reported in our previous work (Yang, Lamochi Roozalipour et al., 2021). Vicilin and albumins were able to form stiffer interfaces, and their interfacial microstructure was affected by the applied deformations.

Frequency sweeps (data not shown) were used to further investigate the interfacial properties. The frequency dependence of the dilatational storage modulus showed power-law behaviour, i.e. $E_d' \sim \omega^n$. All n-values were between 0.08 and 0.15 (Table 2), revealing a power-law behaviour and weak frequency dependence, which was previously observed for soft solid-like structures (Jaishankar & McKinley, 2012). Additionally, n-values were far lower than 0.5, which implies that the elasticity of the surface is not determined by the exchange of material between the interface and the bulk (Lucassen & Van Den Tempel, 1972). Other mechanisms play a larger role, such as in-plane interactions and momentum transfer between interface and the adjoining bulk phases.

Table 2
The n-value obtained from frequency sweeps on the BGN-protein-stabilised interfaces.[a] Values are presented as mean ± standard deviations; means within a row with the same superscript letter are not significantly different (p > 0.05).

	n-value
EP-BGC	0.08 ± 0.01[a]
MP-BGC	0.08 ± 0.01[a]
VIC-RF	0.15 ± 0.02[c]
LEG-RF	0.12 ± 0.03[bc]
ALB-RF	0.09 ± 0.01[ab]

These observations for the frequency dependence in combination with a value for E_d' which was significantly higher than E_d'' in the amplitude sweeps, implies that all BGN-protein extract-stabilised interfaces behave as viscoelastic disordered solid-like materials, as also previously demonstrated for rapeseed protein-stabilised interfaces (Yang et al., 2020). The interactions on the interface can be further evaluated by analysing the non-linearities in the response. The decline in E_d' suggests changes in the interfacial microstructure, which reveals that the deformations are in the non-linear viscoelastic regime (NLVE). Higher-order harmonics exist in the NLVE, and are not incorporated in the calculation of the value of E_d', as only the intensity and phase of the first harmonic of the Fourier spectrum is used to determine E_d'. The use of the first harmonic is fine for small deformations, as non-linearities and higher harmonics are negligible. The non-linearities start to increase at large deformations, which can be analysed by using Lissajous plots (Ewoldt, Hosoi, & McKinley, 2007). Lissajous plots are graphs that can show the relationship between multiple harmonic signals, in this case, the change in surface pressure versus deformation.

3.5.3. Lissajous plots

Lissajous plots of all BGN protein extract-stabilised interfaces are shown in Fig. 6. At 5% deformation, the plots for EP- and MP-BGC were nearly symmetric, as the plots are similar in the extension and compression part of the cycle. The plots are also relatively narrow, which indicates a predominantly elastic response. The degree of asymmetry started to increase upon larger deformations. At 30% deformation, the plots of EP- and MP-BGC stabilised interfaces became marginally wider, and slightly higher surface pressures are reached at the end of the compression cycle (deformation of −0.30). The minor changes in the Lissajous plot of 30% compared to 5% deformation indicate weak in-plane interactions among adsorbed proteins, which would result in an easily stretchable interfacial layer, as was expected based on their nearly amplitude-independent surface elastic dilatational moduli. LEG-RF stabilised interfaces showed remarkably similar plots in comparison to the EP- and MP-BGC. In addition to the mechanical properties, LEG-RF and the BGCs also had comparable surface activity. This would imply that legumins are dictating the interfacial properties in both EP- and MP-BGC.

The VIC-RF and ALB-RF stabilised interfaces showed substantially different Lissajous plots compared to the legumin-dominated interfaces. At 30% deformation, a steep increase in surface pressure from the bottom-left corner was observed (start extension cycle), representing an elastic response. The curve started to flatten after this point, which indicates intra-cycle strain softening in extension. This phenomenon was most pronounced for the ALB-RF stabilised interface with a nearly horizontal curve between 0.10 and 0.30 deformation. Such behaviour can be attributed to a combination of interfacial network disruption and a decrease in surface density, as the interfacial layer is stretched upon extension. For large deformations, such as 30%, the latter effect most likely dominates in the second half of the extension cycle, leading to a very low slope in that part of the cycle. An opposite behaviour is observed upon compression, as the plots had a higher surface pressure, up to −21 mN/m, at maximum compression, compared to +9 mN/m in
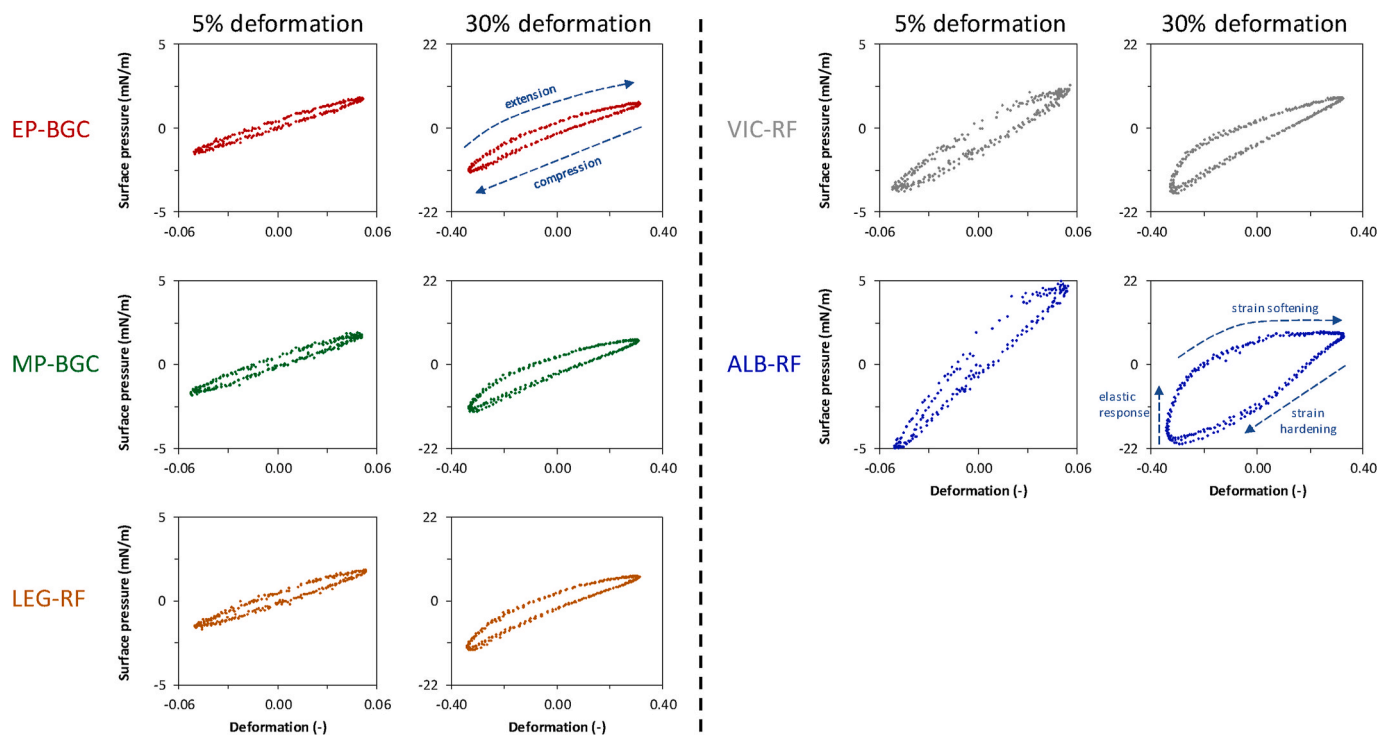
Fig. 6. Lissajous plots of surface pressure as a function of the applied deformation, obtained from amplitude sweeps of air-water interfaces stabilised by BGN protein extracts: extensively (EP-BGC) and mildly (MP-BGC) purified concentrates, vicilin-rich faction (VIC-RF), legumin-rich fraction (LEG-RF) and albumin-rich fraction (ALB-RF). For clarity, one representative plot is shown for each sample, whilst comparable plots were obtained for at least three replicate measurements.

the extension cycle. This indicates intra-cycle strain hardening, which is also affected by a density effect, as the adsorbed material is concentrated upon extensive compression. This could ultimately lead to jamming between the interfacial stabilisers (Yang et al., 2021). The overall behaviour observed in the Lissajous plots of ALB-RF and VIC-RF imply strong in-plane interactions among the adsorbed proteins. ALB-RF had stronger interactions compared to VIC-RF, as the strain hardening in compression and strain softening in compression was most pronounced for ALB-RF.

On the other hand, the legumin-dominated interfaces (EP-BGC, MP-BGC and LEG-RF) were much weaker and more easily stretchable compared to VIC-RF and ALB-RF stabilised interfaces. The quaternary structure of the proteins could largely influence their intermolecular interactions at the surface. Legumins were found to be highly aggregated in light scattering experiments (Fig. 4A), thus may have weaker in-plane interactions at the surface than smaller molecules such as trimeric vicilin or even smaller albumin. This was demonstrated for highly aggregated pea proteins (E. B. A. Hinderink, Sagis, Schroën, & Berton-Carabin, 2020). The albumins also had a zeta-potential of −3.3 mV, whilst the other proteins had a value of at least −9.5 mV. The zeta potential results from the electrophoretic mobility of the proteins, which are attributed to the protein charges. The small molecular size and low zeta potential of albumins could allow more proteins on the surface to closely approach each other, which will definitely contribute to stronger attractive protein-protein interactions in the interface. Another factor could be the presence of disulphide bonds, which are present in albumins shown by the SDS-PAGE experiments, where the albumins dissociated under reducing conditions (Souza, 2020). For whey protein β-lactoglobulin, it is often assumed that disulphide bonds can interact at the surface and form a strong and highly interconnected network, which might also be the case for plant albumins (Rousseau, Madadlou, Floury, & Dupont, 2020). In our previous work, we have demonstrated that pea albumins were able to form a denser and better interconnected microstructure compared to pea globulins (Yang et al.,).

3.5.4. Step-dilatational behaviour

The relaxation behaviour of the interfaces was studied by performing step-dilatation experiments. Briefly, the area of the droplet was suddenly deformed and kept constant after deformation. As a result, a relaxation response of the surface stress (γ) as a function of time (t) could be obtained. An example of the relaxation response is shown in Fig. S3 in the SI. This response was fitted to the following equation:

$$\gamma(t) = ae^{-(t/\tau_1)^\beta} + be^{-t/\tau_2} + c$$

The equation contains a Kohlraus-William-Watts stretched exponential, which has previously been used to study dynamic heterogeneity in the relaxation response of interfaces (Sagis et al., 2019), and is described in terms of the stretch component β and the relaxation time τ_1. The second exponential term was added to include the influence of ageing of the interface during the relaxation process, and is described by the characteristic time τ_2. We will further elaborate on the β and τ_1 (Table 3), as these values are directly related to the relaxation response. Other fitting parameters can be found in Table S2 in the SI.

A β-value <1 indicates dynamic heterogeneity, which can be related

Table 3
β and τ_1 obtained from step-dilatation experiments of air-water interfaces stabilised by BGN protein extracts: extensively (EP-BGC) and mildly (MP-BGC) purified concentrates, vicilin-rich faction (VIC-RF), legumin-rich fraction (LEG-RF) and albumin-rich fraction (ALB-RF).a

	Compression		Extension	
	B	τ_1 (s)	β	τ_1 (s)
EP-BGC	0.58 ± 0.05^a	26.1 ± 6.7^a	0.53 ± 0.05^a	27.6 ± 5.3^a
MP-BGC	0.62 ± 0.03^a	22.3 ± 6.7^a	0.57 ± 0.07^a	24.6 ± 3.6^a
VIC-RF	0.62 ± 0.01^a	27.4 ± 7.1^a	0.59 ± 0.03^a	19.6 ± 0.9^a
LEG-RF	0.61 ± 0.01^a	21.9 ± 5.4^a	0.57 ± 0.05^a	24.1 ± 7.7^a
ALB-RF	0.62 ± 0.03^a	21.4 ± 3.8^a	0.55 ± 0.01^a	23.0 ± 1.7^a

a Values are presented as mean ± standard deviations; means within a row with the same superscript letter are not significantly different (p > 0.05).

to heterogeneity in the interfacial microstructure. This implies local variations in the relaxation kinetics and a wide spectrum of relaxation times. Dynamic heterogeneity is a known phenomenon in disordered solids (Klafter & Shlesinger, 1986; Sagis et al., 2019). The β-values of all interfaces were between 0.53 and 0.62, and confirms the presence of dynamic heterogeneity. Upon compression, slightly higher β-values were obtained compared to those measured in extension, which could be attributed to the formation of a slightly denser and more homogeneous structure upon compression of the material. In earlier work, similar β-values were obtained for dairy and plant protein-stabilised interfaces, where this dynamic heterogeneity was shown to be related to a heterogeneous interfacial microstructure (Cicuta, 2007; Yang et al., 2020; Yang, Waardenburg, et al., 2021). The relaxation time τ_1 for BGN proteins was also comparable to the values previously reported. From these results, in combination with the frequency and amplitude sweeps, it can be concluded that the BGN protein extract-stabilised interfaces also behave as heterogeneous 2D viscoelastic solids.

3.6. Foaming properties

BGN-protein extract-stabilised foams were studied for their overrun (% foam volume over initial sample volume) and the foam half-life time (time for the initial foam volume to decay by half). At 0.1% (w/w) protein concentration, the EP-BGC-stabilised foams had an overrun of 12%, whilst the MP-BGC had an overrun of 28% (Fig. 7A). At a similar protein concentration, the VIC-RF-stabilised foams had an even lower overrun of 11%, whilst that of LEG-RF had was 35%. The ALB-RF-stabilised foams, in comparison, had a remarkably high overrun of 266%. The higher overrun of ALB-RF could be attributed to the fast increase of surface pressure in the initial phase (first 10 s) of adsorption. ALB-RF was also able to form substantially stiffer and more interconnected interfacial layers compared to VIC-RF and LEG-RF. The interfacial properties of VIC-RF and LEG-RF help us understand the foaming properties. The slow adsorption of VIC-RF towards the air-water interface (2 s lag time) could have resulted in the low foam overrun. In comparison, LEG-RF showed the fastest adsorption at the interface, but formed a much weaker and more easily stretchable interface, so the bubbles could not be effectively stabilised. A higher foam formation for albumins compared to globulins was also observed for sunflower proteins (González-Pérez et al., 2005). We should keep in mind that other properties can also largely influence the foaming properties, such as bulk properties.

The slightly higher overrun for MP-BGC could be attributed to the presence of albumins, which became more evident at a higher protein concentration of 1% (w/w) (Fig. 7A). The overrun of the MP-BGC increased from 28 to 159%, whilst the overrun of the globulin-dominated systems EP-BGC, VIC-RF and LEG-RF were 18, 19 and 109, respectively. The albumins seem to play a key role in the foam formation of MP-BGC, whilst the vicilin seemed to dominate the foaming

properties of the EP-BGC. This might appear contradictory to the drop tensiometer data, where the legumin fraction was found to mainly stabilise the interfaces of the two concentrates. This can be explained by the mechanism of interface formation, which in the drop tensiometer is based on the diffusion of the proteins towards the interface. Additionally, the proteins in the droplet are abundantly present, which allow the legumins to diffuse faster to the air-water interface in comparison to the slower albumins and vicilins. A convectional flow is also present in the foam formation during whipping or sparging, thus allowing the slow adsorbing protein to also adsorb at the interface. In this case, the absolute amount of proteins seems to have a primary influence on the foam formation, with vicilin as the main protein fraction, seemingly dominating the overrun of EP-BGC.

The EP-BGC had a foam half-life time of 4 min at 0.1% (w/w) and 60 min at 1% (w/w) protein concentration, whilst that of MP-BGC were substantially different with 10 min for 0.1% (w/w) and 443 min at 1% (w/w) (Fig. 7B). Also, here the albumins are the key foam stabilisers, as the foam half-life time of 0.1% (w/w) ALB-RF was 314 min, whilst that of VIC-RF and LEG-RF (even at 1% w/w) did not surpass 47 min. The average air bubble size was also studied and shown in Fig. S4 in the SI. At 0.1% (w/w), ALB-RF was the only sample that could form small air bubbles with a size of 0.056 mm, whilst the other protein samples formed air bubbles larger than 0.266 mm. At a higher protein concentration of 1%, the air bubble size of EP-BGC, MP-BGC and LEG-RF decreased to 0.074–0.185 mm, but for EP-BGC, LEG-RF and VIC-RF foam half-life times still remained below 60 min. Normally, small air bubbles with a narrow size distribution would increase the foam stability, as drainage and disproportionation are slowed down and more liquid is entrapped into the foam. This is not observed for the EP-BGC, LEG-RF and VIC-RF-stabilised foams, which could be related to their less stiff and more stretchable interfacial layer compared to ALB-RF. The ALB-RF showed high stability due to the smaller air bubbles, which were stabilised by a stiff interfacial layer. These BGN albumins were also the key foam stabilisers in the 1% (w/w) MP-BGC stabilised foam. Good foaming properties (high overrun and stability) were also observed for albumins from other plant sources such as rapeseed, lentils and pea (Ghumman, Kaur, & Singh, 2016; Lu et al., 2000; Nitecka, Raab, & Schwenke, 1986). It is also worth mentioning that a 0.1% (w/w) WPI-stabilised foam showed a foam half-life time of 258 min, comparable to that of ALB-RF (314 min) (Yang, Lamochi Roozalipour et al., 2021).

Interestingly, the non-proteinaceous components in MP-BGC, such as lipids, phenols and starch, did not negatively influence the foam formation and stability; considering that these components can largely reduce foaming properties (Rodríguez, von Staszewski, & Pilosof, 2015; Wilde et al., 2003). This was especially unusual for the lipids, as the MP-BGC had a lipid content of 10.8%, which are known to destabilise protein foams, by decreasing protein layer formation on the interface (Denkov, 2004). The seemingly lack of influence by the lipids can be
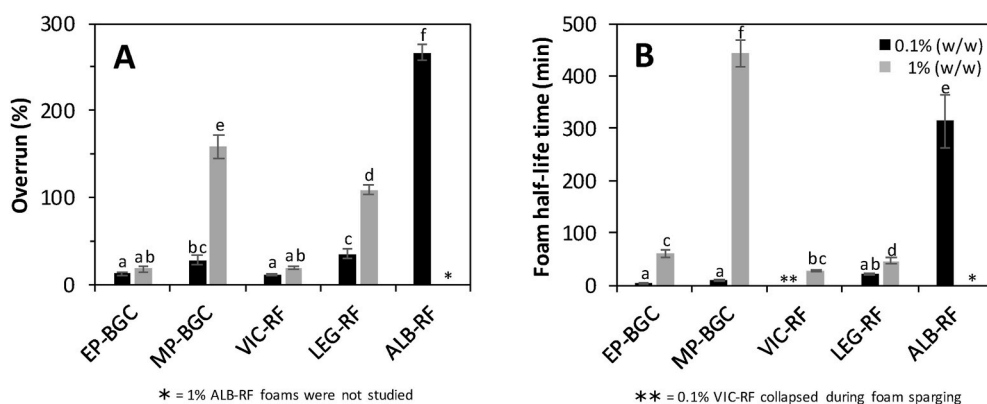
Fig. 7. The foam overrun (A) and foam volume half-life time (B) of foams prepared with BGN protein extracts: extensively (EP-BGC) and mildly (MP-BGC) purified concentrates, vicilin-rich faction (VIC-RF), legumin-rich fraction (LEG-RF) and albumin-rich fraction (ALB-RF). Foams produced from 0.1% (w/w) are indicated in black, and those at 1% (w/w) in grey. The legend in panel B is also valid for panel A. Averages and standard deviations were obtained from at least three measurements.

* = 1% ALB-RF foams were not studied

** = 0.1% VIC-RF collapsed during foam sparging

attributed to the native colloidal state of the lipids, which were present in the form of oleosomes. The triglycerides could be entrapped in the oleosomes, which prevents these lipids from having a destabilising effect on the foams (Yang et al., 2020). We conclude that mild-purification is a suitable method to produce a protein concentrate (MP-BGC) with excellent foaming properties.

3.7. Emulsifying properties

Emulsions were prepared with EP-BGC and MP-BGC in a concentration range of 0.2–2% protein (w/w), and evaluated for the average droplet size ($d_{3,2}$) directly after droplet formation. The single droplet size was also determined by mixing the emulsion with sodium dodecyl sulphate (SDS) to break up potential flocculates. As shown in Fig. 8, the single droplet size increased steeply at protein concentrations below 0.7% (w/w); this concentration region was previously characterised as the protein-poor regime (Delahaije, Gruppen, Giuseppin, & Wierenga, 2015; E.; Hinderink, Münch, Sagis, Schröen, & Berton-Carabin, 2019). In this regime, the MP-BGC-stabilised emulsions had larger single droplet sizes compared to the EP-BGC-stabilised emulsions. MP-BGC emulsions also had larger flocculates (2.4 and 4.0 μm) at protein concentrations below 0.7% (w/w), whilst EP-BGC emulsions only had flocculates of 3.0 μm at 0.2% (w/w) protein concentration. Both BGCs showed no flocculation at a protein concentration higher than 0.7% (w/w), and the $d_{3,2}$ remained constant between 0.58 and 0.88 μm, which indicates the protein-rich regime. From these results, it can be concluded that EP-BGC can form smaller single droplets that flocculate less compared to MP-BGC in the protein-poor regime (<0.7% w/w). On the other hand, both BGCs formed similar size droplets in the protein-rich regime (≥0.7% w/w). The emulsion stability and the influence of the different protein fractions were further evaluated at the critical protein concentration (i.e. 0.7% w/w), which was found between the protein-poor and -rich regime (Sridharan, Meinders, Bitter, & Nikiforidis, 2019).

The droplet size distribution of emulsions stabilised with 0.7% (w/w) BGN protein extract, measured directly after emulsion formation, is shown in Fig. 9. In general, all BGN protein extracts were able to form single oil droplets with a $d_{3,2}$ between 0.64 and 0.85 μm (upon addition of SDS), and several protein extracts showed the presence of larger flocculates. EP-BGC and MP-BGC had comparable peaks with a $d_{3,2}$ of 0.85 μm. After SDS addition, the size distributions remained similar,
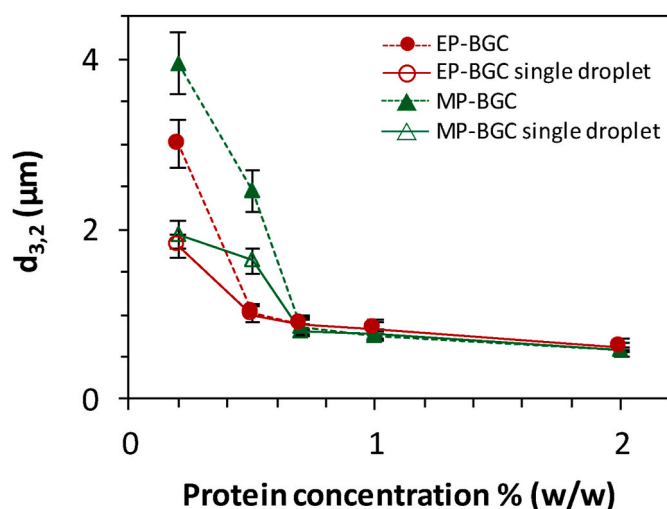
Fig. 8. Average droplet size (d3,2) over protein concentration of 10% (w/w) oil-in-water emulsions prepared with extensively (EP-BGC) and mildly (MP-BGC) purified BGN protein concentrates at various protein concentrations (dotted line). The single droplet size was also studied by breaking up flocculates using SDS (solid line). The data points are the average from two replicates, and the error bars indicate standard deviations.
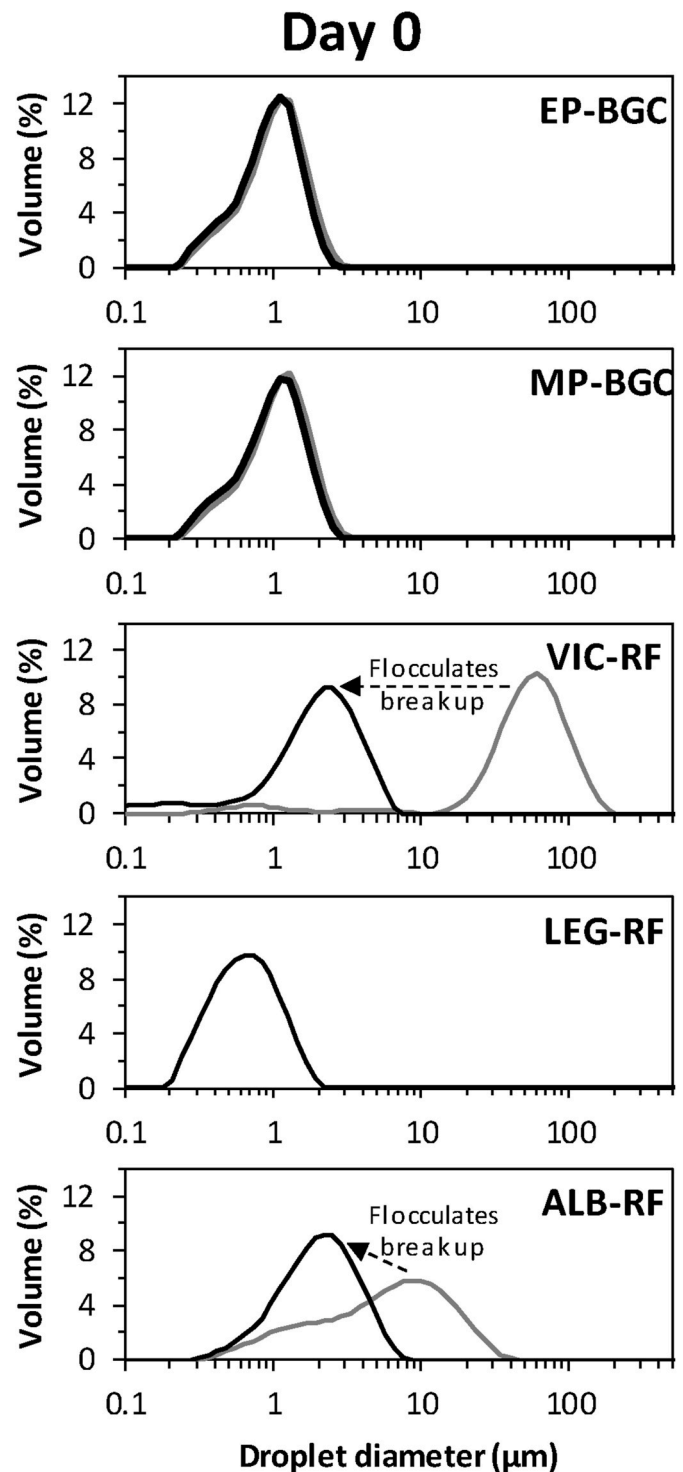
Fig. 9. Droplet size distribution of 10% (w/w) oil-in-water emulsions prepared with BGN protein extracts at 0.7% (w/w) protein concentration, measured directly after emulsion formation (grey line). The size distribution of single droplets after the flocculates were disrupted with SDS were also shown (black line). For clarity, one representative distribution is shown for each sample, but comparable results were obtained on at least two replicates.

which indicated no flocculation in these emulsions. VIC-RF-stabilised emulsions showed a large peak with an average $d_{3,2}$ of 10.4 μm, and 0.75 μm for single droplets, revealing the formation of large flocculates. ALB-RF-stabilised emulsions had a $d_{3,2}$ of 2.5 μm and showed flocculation, which was clearly indicated in the size distribution with peak

heights recorded at 10 μm, and a shoulder peak at the height of the single droplet size ($d_{3,2}$ of 1.4 μm) after addition of SDS. In comparison, emulsion droplets stabilised with LEG-RF showed a narrow droplet size distribution with a $d_{3,2}$ of 0.64 μm and no droplet flocculation.

The stability against flocculation of emulsions prepared with LEG-RF could be attributed to the higher zeta-potential of these proteins (−24.1 mV). The zeta-potential can be related to the charge of the legumin, and imparts a higher charge on the protein interface around an oil droplet, resulting in increased electrostatic repulsion, thus reducing droplet flocculation (Berton-Carabin & Schroën, 2015). The VIC-RF and ALB-RF solutions had a lower zeta-potential of −11.4 and −3.3 mV, respectively, which would result in less electrostatic repulsion between the droplets. The attractive forces overcame these repulsive forces, and the droplets started to flocculate. Interestingly, the zeta-potential of EP-BGC and MP-BGC solutions were −10.5 and −9.5 mV, respectively, which were close to the zeta-potential of VIC-RF. This could be expected, considering that vicilin is the largest protein fraction in both BGC's. However, no flocculation was observed for these emulsions, which indicate that legumins contributed largely to these emulsions through co-adsorption with vicilin and albumins. Besides, the presence of albumins in the protein-poor regime of the MP-BGC could have resulted in the larger droplets and flocculates, since the amount of legumins was insufficient at these concentrations to stabilise the droplets. In the protein-rich regime, more legumin was present in the MP-BGC, thus resulted in stable emulsions.

The stability of the droplets was further evaluated by measuring the droplet size after 1 and 7 days. Emulsions stabilised with EP-BGC, MP-BGC, and LEG-RF had similar droplet size distributions after 7 days of storage (see Fig. S5 in SI). After 7 days, the emulsions remained stable against creaming. This stability was not observed for ALB-RF and VIC-RF-stabilised emulsions, as both emulsions had a shift towards the right of their size distribution curves, which suggests the presence of larger flocculates (Fig. 10). The same observation was made after the addition of SDS, suggesting the increase of single droplets (coalescence), or alternatively, the flocculation of droplets could not be disrupted using SDS. Microscopy images of these samples revealed the presence of some larger structures, which appeared to be flocculated droplets (Fig. 10).

These large flocculates in the emulsions also resulted in creaming, as determined with the creaming index. This was calculated by dividing the height of the serum layer (bottom layer) by the height of the total sample times 100. The creaming index was 44 and 72% for VIC-RF and ALB-RF, respectively. The poorer emulsifying properties of albumins compared to globulins were also found for coconut meat, lentil and horse gram proteins (Ghumman et al., 2016; Patil & Benjakul, 2017). In those studies, the globulins could form smaller and more stable droplets.

In this work, we have shown that the legumins are an important protein fraction to form emulsion droplets that are stable against coalescence, flocculation and creaming. Since legumins are present in both EP-BGC and MP-BGC, both concentrates were able to stabilise emulsions. Also, the non-proteinaceous compounds seemingly did not negatively influence the emulsion formation. Therefore, mild purification is a suitable method to obtain protein concentrates, which can form stable emulsions.

4. Conclusions

In this work, we have investigated the interfacial, foaming and emulsifying properties of Bambara groundnut protein extracts, obtained using either an extensive or mild purification method, which yielded protein concentrates containing vicilin and legumin proteins. A major compositional difference between the two concentrates was the presence of albumins, and more non-proteinaceous compounds (lipids, phenols, starch) in the mildly purified protein extract. The legumin in both protein extracts was the dominating air-water interface stabilising protein, forming weak and mobile interfaces. An important finding was the ability of the albumins to form stiff viscoelastic solid-like interfaces. The albumins also possess promising foaming properties with high foamability and stability. They resulted in better foaming properties for the mildly purified protein concentrate (9x higher foamability and 8x higher stability) compared to the concentrate obtained from extensive purification, where albumins were absent. On the other hand, albumins were less suitable to stabilise emulsion droplets against flocculation due to their low charge. For emulsions, legumin played a major role in forming stable emulsions for both the extensive and mild-purified
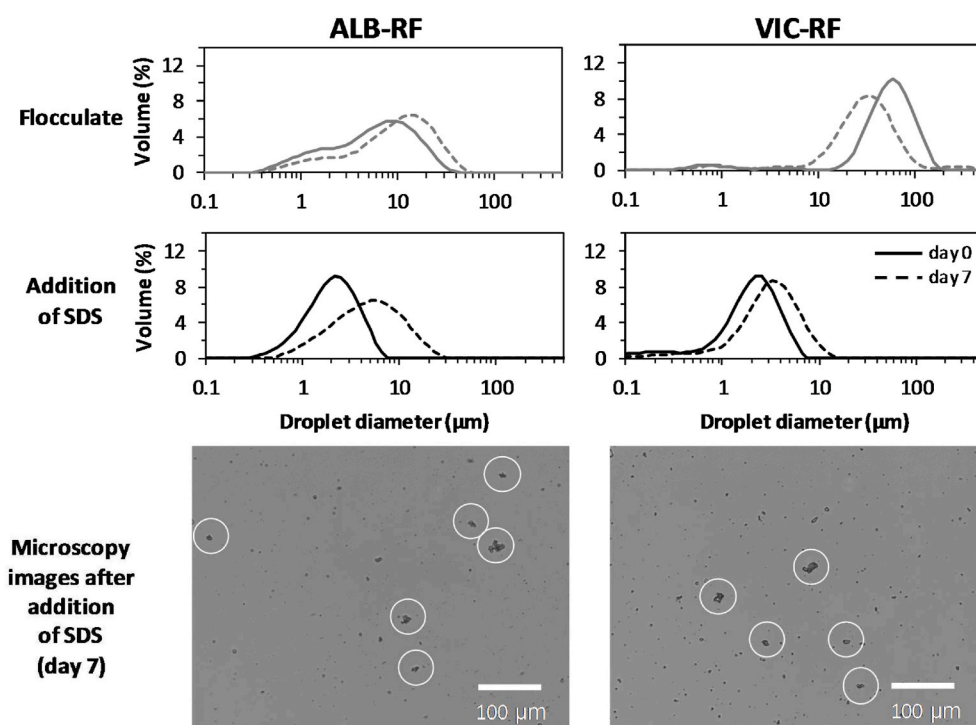

Fig. 10. Droplet size distribution of 10% (w/w) oil-in-water emulsions prepared with the albumin-rich (ALB-RF) and vicilin-rich (VIC-RF) fraction, measured directly after emulsion formation (solid line) and after 7 days of storage at 4 °C (dotted line). Single droplets were also measured after disruption of flocculates. For clarity, one representative measurement was shown for each sample, whilst comparable results were obtained on at least two replicates. Microscopy images of both emulsions on day 7 after addition of SDS were also shown. Irreversibly aggregated flocculates were marked with circles.

protein concentrates. Both extracts were able to form stable emulsions in the protein-rich regime ($\geq$0.7% w/w). Additionally, the mildly purified protein concentrate with a higher amount of lipids and phenols outperformed the extensively purified concentrate in terms of foaming properties, mainly due to the presence of albumins. Generally, albumins are discarded in the conventional extensive purification method, whilst these proteins remain in the extract when using the milder processing method on the plant sources. The findings in our work show that the type of extraction process can influence the functional properties of the protein extract; with a more sustainable and mild purification method being suitable for the production of a highly functional protein extract from Bambara groundnut. These mild types of methods should be further explored to increase the sustainability aspect of plant-based ingredients.

CRediT authorship contribution statement

Jack Yang: Conceptualization, Methodology, Investigation, Validation, Visualization, Writing – original draft. **Annemiek de Wit:** Methodology, Investigation. **Claudine F. Diedericks:** Conceptualization, Methodology, Investigation, Writing – review & editing. **Paul Venema:** Writing – review & editing. **Erik van der Linden:** Writing – review & editing, Funding acquisition. **Leonard M.C. Sagis:** Conceptualization, Methodology, Supervision, Writing – review & editing.

Declaration of competing interest

The authors have declared that no competing interest exist. This manuscript has not been published and is not under consideration for publication in any other journal. All authors approve this manuscript and its submission to Food Hydrocolloids.

Acknowledgements

Appendix A. Supplementary data

Supplementary data to this article can be found online at https://doi. org/10.1016/j.foodhyd.2021.107190.

References

Adebowale, Y. A., Schwarzenbolz, U., & Henle, T. (2011). Protein isolates from Bambara groundnut (Voandzeia Subterranean L.): Chemical characterization and functional properties. *International Journal of Food Properties, 14*(4), 758–775. https://doi.org/10.1080/10942910903420743

Adeleke, O. R., Adiamo, O. Q., & Fawale, O. S. (2018). Nutritional, physicochemical, and functional properties of protein concentrate and isolate of newly-developed Bambara groundnut (Vigna subterrenea L.) cultivars. *Food Science and Nutrition, 6*(1), 229–242. https://doi.org/10.1002/fsn3.552

Arise, A. K., Nwachukwu, I. D., Aluko, R. E., & Amonsou, E. O. (2017). Structure, composition and functional properties of storage proteins extracted from Bambara groundnut (Vigna subterranea) landraces. *International Journal of Food Science and Technology, 52*(5), 1211–1220. https://doi.org/10.1111/ijfs.13386

Barac, M., Cabrilo, S., Pesic, M., Stanojevic, S., Zilic, S., Macej, O., et al. (2010). Profile and functional properties of seed proteins from six pea (Pisum sativum) genotypes. *International Journal of Molecular Sciences, 11*(12), 4973–4990. https://doi.org/10.3390/ijms11124973

Berton-Carabin, C. C., & Schroën, K. (2015). Pickering emulsions for food applications: Background, trends, and challenges. *Annual Review of Food Science and Technology, 6*, 263–297. https://doi.org/10.1146/annurev-food-081114-110822

Cao, Y., Xiong, Y. L., Cao, Y., & True, A. D. (2018). Interfacial properties of whey protein foams as influenced by preheating and phenolic binding at neutral pH. *Food Hydrocolloids, 82*, 379–387. https://doi.org/10.1016/j.foodhyd.2018.04.020

Chéreau, D., Videcoq, P., Ruffieux, C., Pichon, L., Motte, J. C., Belaid, S., et al. (2016). Combination of existing and alternative technologies to promote oilseeds and pulses proteins in food applications. *OCL - Oilseeds and Fats, Crops and Lipids, 41*(1). https://doi.org/10.1051/ocl/2016020

Cicuta, P. (2007). Compression and shear surface rheology in spread layers of β-casein and β-lactoglobulin. *Journal of Colloid and Interface Science, 308*(1), 93–99. https://doi.org/10.1016/j.jcis.2006.12.056

Das Purkayastha, M., Gogoi, J., Kalita, D., Chattopadhyay, P., Nakhuru, K. S., Goyary, D., et al. (2014). Physicochemical and functional properties of rapeseed protein isolate: Influence of antinutrient removal with acidified organic solvents from rapeseed meal. *Journal of Agricultural and Food Chemistry, 62*(31), 7903–7914. https://doi.org/10.1021/jf5023803

Delahaije, R. J. B. M., Gruppen, H., Giuseppin, M. L. F., & Wierenga, P. A. (2015). Towards predicting the stability of protein-stabilized emulsions. *Advances in Colloid and Interface Science, 219*, 1–9. https://doi.org/10.1016/j.cis.2015.01.008

Denkov, N. D. (2004). Mechanisms of foam destruction by oil-based antifoams. *Langmuir, 20*(22), 9463–9505. https://doi.org/10.1021/la0496760

Diedericks, C. F., de Koning, L., Jideani, V. A., Venema, P., & van der Linden, E. (2019). Extraction, gelation and microstructure of Bambara groundnut vicilins. *Food Hydrocolloids, 97*, 105226. https://doi.org/10.1016/j.foodhyd.2019.105226

Diedericks, C. F., Shek, C., Jideani, V. A., & Venema, P. (2020). Physicochemical properties and gelling behaviour of Bambara groundnut protein isolates and protein-enriched fractions. *Food Research International*. https://doi.org/10.1016/j.foodres.2020.109773, 109773.

Diedericks, C. F., Venema, P., Mubaiwa, J., Jideani, V. A., & van der Linden, E. (2020). Effect of processing on the microstructure and composition of Bambara groundnut (Vigna subterranea (L.) Verdc.) seeds, flour and protein isolates. *Food Hydrocolloids, 108*, 106031. https://doi.org/10.1016/j.foodhyd.2020.106031

Ewoldt, R. H., Hosoi, A. E., & McKinley, G. H. (2007). New measures for characterizing nonlinear viscoelasticity in large amplitude oscillatory shear. *Journal of Rheology, 52*(6), 1427–1458. https://doi.org/10.1122/1.2970095

Geerts, M. E. J., Nikiforidis, C. V., van der Goot, A. J., & van der Padt, A. (2017). Protein nativity explains emulsifying properties of aqueous extracted protein components from yellow pea. *Food Structure, 14*, 104–111. https://doi.org/10.1016/j.foostr.2017.09.001

Ghumman, A., Kaur, A., & Singh, N. (2016). Functionality and digestibility of albumins and globulins from lentil and horse gram and their effect on starch rheology. *Food Hydrocolloids, 61*, 843–850. https://doi.org/10.1016/j.foodhyd.2016.07.013

Gonzalez-Perez, S., & Vereijken, J. M. (2007). Sunflower proteins: Overview of their physicochemical, structural and functional properties. *Journal of the Science of Food and Agriculture, 87*, 2173–2191. https://doi.org/10.1002/jsfa

Gonzalez-Perez, S., Vereijken, J. M., van Koningsveld, G. A., Gruppen, H., & Voragen, A. G. J. (2005). Physicochemical Properties of 2S albumins and the corresponding protein isolate from Sunflower (Helianthus annuus). *Food Chemistry and Toxicology, 70*(1), C98–C103.

González-Pérez, S., Vereijken, J. M., Van Koningsveld, G. A., Gruppen, H., & Voragen, A. G. J. (2005). Formation and stability of foams made with sunflower (Helianthus annuus) proteins. *Journal of Agricultural and Food Chemistry, 53*(16), 6469–6476. https://doi.org/10.1021/jf0501793

Guéguen, J., Popineau, Y., Anisimova, I. N., Fido, R. J., Shewry, P. R., & Tatham, A. S. (1996). Functionality of the 2S albumin seed storage proteins from sunflower (Helianthus annuus L.). *Journal of Agricultural and Food Chemistry, 44*(5), 1184–1189. https://doi.org/10.1021/jf950683f

Harris, T., Jideani, V., & Le Roes-Hill, M. (2018). Flavonoids and tannin composition of Bambara groundnut (Vigna subterranea) of Mpumalanga, South Africa. *Heliyon, 4*(9), Article e00833. https://doi.org/10.1016/j.heliyon.2018.e00833

Hinderink, E., Münch, K., Sagis, L., Schröen, K., & Berton-Carabin, C. C. (2019). *Synergistic stabilisation of emulsions by blends of dairy and plant proteins: Contribution of the interfacial composition*. Submitted: Food Hydrocolloids. https://doi.org/10.1016/j.foodhyd.2019.105206, 105206.

Hinderink, E. B. A., Sagis, L., Schroën, K., & Berton-Carabin, C. C. (2020). Behavior of plant-dairy protein blends at air-water and oil-water interfaces. *Colloids and Surfaces B: Biointerfaces, 192*, 111015. https://doi.org/10.1016/j.colsurfb.2020.111015

Jaishankar, A., & McKinley, G. H. (2012). Power-law rheology in the bulk and at the interface: Quasi-properties and fractional constitutive equations. *Proceedings of the Royal Society A, 469*(2149). https://doi.org/10.1098/rspa.2012.0284, 20120284–20120284.

Jiang, J., Chen, J., & Xiong, Y. L. (2009). Structural and emulsifying properties of soy protein isolate subjected to acid and alkaline pH-shifting processes. *Journal of Agricultural and Food Chemistry, 57*(16), 7576–7583. https://doi.org/10.1021/jf901585n

Jin, X. L., Wei, X., Qi, F. M., Yu, S. S., Zhou, B., & Bai, S. (2012). Characterization of hydroxycinnamic acid derivatives binding to bovine serum albumin. *Organic and Biomolecular Chemistry, 10*(17), 3424–3431. https://doi.org/10.1039/c2ob25237f

Keppler, J. K., Schwarz, K., & van der Goot, A. J. (2020). Covalent modification of food proteins by plant-based ingredients (polyphenols and organosulphur compounds): A commonplace reaction with novel utilization potential. *Trends in Food Science & Technology, 101*, 38–49. https://doi.org/10.1016/j.tifs.2020.04.023

Klafter, J., & Shlesinger, M. F. (1986). On the relationship among three theories of relaxation in disordered. *Proceedings of the National Academy of Sciences of the United States of America, 83*(4), 848–851. https://doi.org/10.1073/pnas.83.4.848

Kornet, C., Venema, P., Nijsse, J., van der Linden, E., van der Goot, A. J., & Meinders, M. (2020). Yellow pea aqueous fractionation increases the specific volume fraction and viscosity of its dispersions. *Food Hydrocolloids, 99*, 105332. https://doi.org/10.1016/j.foodhyd.2019.105332

Lucassen, J., & Van Den Tempel, M. (1972). Dynamic measurements of dilational properties of a liquid interface. *Chemical Engineering Science, 27*(6), 1283–1291. https://doi.org/10.1016/0009-2509(72)80104-0

Lu, B. Y., Quillien, L., & Popineau, Y. (2000). Foaming and emulsifying properties of pea albumin fractions and partial characterisation of surface-active components. *Journal of the Science of Food and Agriculture, 80*(13), 1964–1972. https://doi.org/10.1002/1097-0010(200010)80:13<1964::AID-JSFA737>3.0.CO;2-J

Mubaiwa, J., Fogliano, V., Chidewe, C., & Linnemann, A. R. (2017). Hard-to-cook phenomenon in Bambara groundnut (Vigna subterranea (L.) Verdc.) processing: Options to improve its role in providing food security. *Food Reviews International, 33*(2), 167–194. https://doi.org/10.1080/87559129.2016.1149864

Mubaiwa, J., Fogliano, V., Chidewe, C., & Linnemann, A. R. (2018). Bambara groundnut (vigna subterranea (L.) Verdc.) flour: A functional ingredient to favour the use of an unexploited sustainable protein source. *PloS One, 13*(10), 1–19. https://doi.org/10.1371/journal.pone.0205776

Murevanhema, Y. Y., & Jideani, V. A. (2013). Potential of Bambara groundnut (vigna subterranea (L.) Verdc) milk as a probiotic beverage-A review. *Critical Reviews in Food Science and Nutrition, 53*(9), 954–967. https://doi.org/10.1080/10408398.2011.574803

Nikiforidis, C. V. (2019). Structure and functions of oleosomes (oil bodies). *Advances in Colloid and Interface Science, 274*, 102039. https://doi.org/10.1016/j.cis.2019.102039

Nitecka, E., Raab, B., & Schwenke, K. D. (1986). Chemical modification of proteins. Part 12. Effect of succinylation on some physico???chemical and functional properties of the albumin fraction from rapeseed (Brassica napus L.). *Food, 30*(10), 975–985. https://doi.org/10.1002/food.19860301003

Ntone, E., Bitter, J. H., & Nikiforidis, C. V. (2020). Not sequentially but simultaneously: Facile extraction of proteins and oleosomes from oilseeds. *Food Hydrocolloids, 102*, 105598. https://doi.org/10.1016/j.foodhyd.2019.105598

Ntone, E., Wesel, T. Van, Sagis, L. M. C., Meinders, M., Bitter, J. H., & Nikiforidis, C. V. (2021). Adsorption of rapeseed proteins at oil/water interfaces . Janus-like napins dominate the interface. *Journal of Colloid and Interface Science, 583*, 459–469. https://doi.org/10.1016/j.jcis.2020.09.039

Osborne, T. B. (1924). *The vegetable proteins*. Longmans green and co.

Patil, U., & Benjakul, S. (2017). Characteristics of albumin and globulin from coconut meat and their role in emulsion stability without and with proteolysis. *Food Hydrocolloids, 69*, 220–228. https://doi.org/10.1016/j.foodhyd.2017.02.006

Rodríguez, S. D., von Staszewski, M., & Pilosof, A. M. R. (2015). Green tea polyphenols-whey proteins nanoparticles: Bulk, interfacial and foaming behavior. *Food Hydrocolloids, 50*, 108–115. https://doi.org/10.1016/j.foodhyd.2015.04.015

Rousseau, F., Madadlou, A., Floury, J., & Dupont, D. (2020). Interfacial and (emulsion) gel rheology of hydrophobized whey proteins. *Food Hydrocolloids, 100*. https://doi.org/10.1016/j.idairyj.2019.104556

Sagis, L. M. C., Liu, B., Li, Y., Essers, J., Yang, J., Moghimikheirabadi, A., et al. (2019). Dynamic heterogeneity in complex interfaces of soft interface-dominated materials. *Scientific Reports, 9*(1), 1–12. https://doi.org/10.1038/s41598-019-39761-7

Sari, Y. W., Mulder, W. J., Sanders, J. P. M., & Bruins, M. E. (2015). Towards plant protein refinery: Review on protein extraction using alkali and potential enzymatic assistance. *Biotechnology Journal, 10*(8), 1138–1157. https://doi.org/10.1002/biot.201400569

Shahidi, F., & Senadheera, R. (2019). Encyclopedia of food chemistry: Protein–phenol interactions. In *, Vol. 2. Encyclopedia of food chemistry*. Elsevier. https://doi.org/10.1016/b978-0-08-100596-5.21485-6.

Souza, P. F. N. (2020). The forgotten 2S albumin proteins: Importance, structure, and biotechnological application in agriculture and human health. *International Journal of Biological Macromolecules, 164*, 4638–4649. https://doi.org/10.1016/j.ijbiomac.2020.09.049

Sridharan, S., Meinders, M. B. J., Bitter, J. H., & Nikiforidis, C. V. (2019). Native pea flour as stabilizer of oil-in-water emulsions: No protein purification necessary. *Food Hydrocolloids, 101*, 105533. https://doi.org/10.1016/j.foodhyd.2019.105533

Wilde, P. J., Wilde, P. J., Husband, F. a, Husband, F. a, Cooper, D., Cooper, D., et al. (2003). Destabilization of beer foam by lipids: Structural and interfacial effects. *Journal of the American Society of Brewing Chemists, 61*, 196–202. https://doi.org/10.1094/ASBCJ-61-0196

Yang, J., Faber, I, Berton-Carabin, C. C., Nikiforidis, C. V., van der Linden, E., & Sagis, L. M. C. (2020). Foams and air-water interfaces stabilised by mildly purified rapeseed proteins after defatting. *Food Hydrocolloids, 112*, 106270. https://doi.org/10.1016/j.foodhyd.2020.106270

Yang, J., Kornet, R., Diedericks, C. F., Yang, Q., Berton-carabin, C. C., Nikiforidis, C. V., … Sagis, L. M. C. (n.d.). Rethinking plant protein extraction - plant albumins an excellent foaming agent. Under Review.

Yang, J., Lamochi Roozalipour, S. P., Berton-Carabin, C. C., Nikiforidis, C. V., van der Linden, E., & Sagis, L. M. C. (2021). Air-water interfacial and foaming properties of whey protein - sinapic acid mixtures. *Food Hydrocolloids, 112*, 106467. https://doi.org/10.1016/j.foodhyd.2020.106467

Yang, J., Waardenburg, L. C., Berton-Carabin, C. C., Nikiforidis, C. V., van der Linden, E., & Sagis L, M. C. (2021). Air-water interfacial behaviour of whey protein and rapeseed oleosome mixtures. *Journal of Colloid and Interface Science, 602*, 207–221. https://doi.org/10.1016/j.jcis.2021.05.172